

Exact solutions for Big Bounce in loop quantum cosmology

Jakub Mielczarek*

*Astronomical Observatory, Jagiellonian University, 30-244 Kraków, Orla 171, Poland and
The Niels Bohr Institute, Copenhagen University,
Blegdamsvej 17, DK-2100 Copenhagen, Denmark*

Tomasz Stachowiak†

Astronomical Observatory, Jagiellonian University, 30-244 Kraków, Orla 171, Poland

Marek Szydłowski‡

*Department of Theoretical Physics, Catholic University of Lublin, Al. Racławickie 14, 20-950 Lublin, Poland and
Marc Kac Complex Systems Research Centre, Jagiellonian University, Reymonta 4, 30-059 Kraków, Poland*

In this paper we study the flat ($k = 0$) cosmological FRW model with holonomy corrections of Loop Quantum Gravity. The considered universe contains a massless scalar field and the cosmological constant Λ . We find analytical solutions for this model in different configurations and investigate its dynamical behaviour in the whole phase space. We show the explicit influence of Λ on the qualitative and quantitative character of solutions. Even in the case of positive Λ the oscillating solutions without the initial and final singularity appear as a generic case for some quantisation schemes.

I. INTRODUCTION

In recent years Loop Quantum Cosmology (LQC) has inspired realisation of the cosmological scenario in which the initial singularity is replaced by the bounce. In this picture, the Universe is initially in the contracting phase, reaches the minimal, nonzero volume and, thanks to quantum repulsion, evolves toward the expanding phase. Such a scenario has been extensively studied with use of the numerical methods [1, 2]. However, as it was shown for example in [3] exact solutions for bouncing universe with dust and cosmological constant can be found. The aim of the present paper is to show that analytical solutions can also be obtained for the bouncing models arising from LQC. The main advantage of such exact solutions is that they allow for investigations in whole ranges of the parameter domains.

In this paper we consider the flat FRW model with a free scalar field and with the cosmological constant. Quantum effects are introduced in terms of correction to the classical theory. Generally one considers two types of quantum correction: correction from inverse volume and holonomy corrections. The leading effect of the volume corrections is the appearance of the super-inflationary phase. The effect of holonomy corrections, on the other hand, is the appearance of a bounce instead of singularity. The aim of this paper is to investigate analytically these effects in a flat FRW model. That is to say, we neglect corrections from inverse volume, these effects however, has been extensively studied elsewhere. Moreover, these two types of corrections are not equally

important in the same regimes. The inverse volume corrections are mainly important for small values of the scale factor, whereas holonomy corrections are mainly important for large values of the Hubble parameter. In other words, when the minimal scale factor (during the bounce) is large enough, the effects of inverse volume corrections can be neglected.

The flat FRW model in the Loop Quantum Cosmology has been first investigated in the pioneer works of Bojowald [5, 6] and later improved in the works of Ashtekar, Pawłowski and Singh [2, 4, 7]. Bojowald's original description of the quantum universe in currently explored in the number of works and regarded as a parallel line of research [9, 10]. In the present paper, we restrict ourselves to the flat FRW models arising in the framework proposed by Ashtekar and co-workers. Beside the flat models this approach has also been applied to the FRW $k = \pm 1$ models in [8, 11, 12, 13] and Bianchi I in [14, 15]. In these models the unambiguity in the choice of the elementary area for the holonomy corrections appear. In the present paper we consider two kind of approaches to this problem: the so called $\bar{\mu}$ -scheme and μ_0 -scheme (for a more detailed description see Appendix A). We find analytical solutions for the considered models in these two schemes.

The Hamiltonian of the considered model is given by

$$H_{\text{eff}} = -\frac{3}{8\pi G\gamma^2} \sqrt{|p|} \left[\frac{\sin(\bar{\mu}c)}{\bar{\mu}} \right]^2 + \frac{1}{2} \frac{p_\phi^2}{|p|^{3/2}} + |p|^{3/2} \frac{\Lambda}{8\pi G}. \quad (1)$$

In Appendix A we show the derivation of this Hamiltonian in the Loop Quantum Gravity setting. The canonical variables for the gravitational field are (c, p) and for the scalar field (ϕ, p_ϕ) . The canonical variables for the gravitational field can be expressed in terms of the standard FRW variables $(c, |p|) = (\gamma\dot{a}V_0^{1/3}, a^2V_0^{2/3})$. Where the factor γ is called Barbero-Immirzi parameter and is a

*Electronic address: jakubm@poczta.onet.pl

†Electronic address: toms@oa.uj.edu.pl

‡Electronic address: uoszydlo@cyf-kr.edu.pl

constant of the theory, and V_0 is the volume of the fiducial cell. The volume V_0 is just a scaling factor and can be chosen arbitrarily in the domain $V_0 \in \mathbb{R}_+$. Since p is the more natural variable than a here, we present mostly $p(t)$ in the figures. a is always the positive square root of p so the shape of the graphs would be essentially the same when drawn with a . The equations of motions can now be derived with the use of the Hamilton equation

$$\dot{f} = \{f, H_{\text{eff}}\} \quad (2)$$

where the Poisson bracket is defined as follows

$$\begin{aligned} \{f, g\} &= \frac{8\pi G\gamma}{3} \left[\frac{\partial f}{\partial c} \frac{\partial g}{\partial p} - \frac{\partial f}{\partial p} \frac{\partial g}{\partial c} \right] \\ &+ \left[\frac{\partial f}{\partial \phi} \frac{\partial g}{\partial p_\phi} - \frac{\partial f}{\partial p_\phi} \frac{\partial g}{\partial \phi} \right]. \end{aligned} \quad (3)$$

From this definition we can immediately retrieve the elementary brackets

$$\{c, p\} = \frac{8\pi G\gamma}{3} \quad \text{and} \quad \{\phi, p_\phi\} = 1. \quad (4)$$

With use of the Hamiltonian (1) and equation (2) we obtain equations of motion for the canonical variables

$$\begin{aligned} \dot{p} &= \frac{2}{\gamma} \frac{\sqrt{|p|}}{\bar{\mu}} \sin(\bar{\mu}c) \cos(\bar{\mu}c), \\ \dot{c} &= -\frac{1}{\gamma} \frac{\partial}{\partial p} \left\{ \sqrt{|p|} \left[\frac{\sin(\bar{\mu}c)}{\bar{\mu}} \right]^2 \right\} \\ &- \text{sgn}(p) \frac{\kappa\gamma}{4} \frac{p_\phi^2}{|p|^{5/2}} + \text{sgn}(p) \frac{\Lambda\gamma}{2} \sqrt{|p|}, \\ \dot{\phi} &= |p|^{-3/2} p_\phi, \\ \dot{p}_\phi &= 0, \end{aligned} \quad (5)$$

where $\kappa = 8\pi G$. The Hamiltonian constraint $H_{\text{eff}} = 0$ implies

$$\frac{1}{\gamma^2 |p|} \left[\frac{\sin(\bar{\mu}c)}{\bar{\mu}} \right]^2 = \frac{\kappa}{3} \frac{1}{2} \frac{p_\phi^2}{|p|^3} + \frac{\Lambda}{3}. \quad (6)$$

The variable $\bar{\mu}$ corresponds to the dimensionless length of the edge of the elementary loop and can be written in the general form

$$\bar{\mu}(p) = \xi |p|^n \quad (7)$$

where $-1/2 \leq n \leq 0$ and ξ is a constant $\xi > 0$ (this comes from the fact that μ is positively defined). The choice of n and ξ depends on the particular scheme in the holonomy corrections. In particular, boundary values correspond to the cases when $\bar{\mu}$ is the physical distance ($n = -1/2$, $\bar{\mu}$ -scheme) and coordinate distance ($n = 0$, μ_0 -scheme). However, the $n = 0$ case does not lead to the correct classical limit. When $n > 0$, the classical limit

can not be recovered either. Only for negative values of n is the classical limit $p \rightarrow \infty$ correctly recovered

$$\lim_{p \rightarrow \infty} \frac{\sin(\bar{\mu}(p)c)}{\bar{\mu}(p)} = c. \quad (8)$$

Strict motivation of the domain of the parameter n comes from the investigation of the lattice states [25]. The number of the lattice blocks is expressed as $\mathcal{N} = V_0/l_0^3$ where l_0 is the average length of the lattice edge. This value is connected to the earlier introduced length $\bar{\mu}$, namely $\mathcal{N} = \bar{\mu}^{-3}(p)$. During evolution the increase of the total volume is due to the increase of the spin labels on the graph edges or due to the increase of the number of vortices. In this former case the number of the lattice blocks is constant during evolution, $\mathcal{N} = \text{const}$. Otherwise, when the spin labels do not change, the number of vortices scales with the volume, $\mathcal{N} \propto |p|^{3/2}$. The physical evolution correspond to something in the middle, it means the power index lies in the range $[0, 3/2]$. Applying the definition of \mathcal{N} we see that the considered boundary values translate to the domain of n introduced earlier, $n \in [-1/2, 0]$. More detailed investigation of the considered ambiguities can be found in the papers [10, 16] and in the Appendix A.

Combining equations (6), (7) and the first one from the set of equations (5) we obtain

$$\begin{aligned} \left(\frac{dp}{dt} \right)^2 &= \Omega_{\text{I}} |p|^{-1} + \Omega_{\text{II}} |p|^2 - \Omega_{\text{III}} |p|^{2n-3} \\ &- \Omega_{\text{IV}} |p|^{2n} - \Omega_{\text{V}} |p|^{2n+3}, \end{aligned} \quad (9)$$

where new parameters are defined as follow

$$\Omega_{\text{I}} = \frac{2}{3} \kappa p_\phi^2, \quad (10)$$

$$\Omega_{\text{II}} = \frac{4}{3} \Lambda, \quad (11)$$

$$\Omega_{\text{III}} = \frac{1}{9} \kappa^2 \gamma^2 \xi^2 p_\phi^4, \quad (12)$$

$$\Omega_{\text{IV}} = \frac{4}{9} \kappa \Lambda p_\phi^2 \gamma^2 \xi^2, \quad (13)$$

$$\Omega_{\text{V}} = \frac{4}{9} \Lambda^2 \gamma^2 \xi^2. \quad (14)$$

Equation (9) is, in fact, a modified Friedmann equation

$$H^2 = \frac{8\pi G_{\text{eff}}}{3} \rho + \frac{\Lambda_{\text{eff}}}{3}, \quad (15)$$

where the effective constants are expressed as follow

$$G_{\text{eff}} = G \left[1 - \frac{\rho}{\rho_c} \right], \quad (16)$$

$$\Lambda_{\text{eff}} = \Lambda \left[1 - 2 \frac{\rho}{\rho_c} - \frac{\Lambda}{\kappa \rho_c} \right], \quad (17)$$

and

$$\rho = \frac{p_\phi^2}{2|p|^3}, \quad (18)$$

$$\rho_c = \frac{3}{\kappa \gamma^2 \bar{\mu}^2 |p|}. \quad (19)$$

We will study the solutions of the equation (9) for both $\bar{\mu}$ -scheme and μ_0 -scheme.

The organisation of the text is the following. In section II we consider models with $\Lambda = 0$. We find solutions of the equations (9) for both $\bar{\mu}$ -scheme and μ_0 -scheme. Next, in section III we add to our considerations a non-vanishing cosmological constant Λ . We carry out an analysis similar to the case without lambda. We find analytical solutions of the equation(9) for $\bar{\mu}$ -scheme. Then, we study the behaviour of this case in μ_0 -scheme. In section V we summarise the results.

II. MODELS WITH $\Lambda = 0$

In this section we begin our considerations with the model without Λ . Equation (9) is then simplified to the form

$$\left(\frac{dp}{dt}\right)^2 = \Omega_I |p|^{-1} - \Omega_{III} |p|^{2n-3}. \quad (20)$$

We solve this equation for both $\bar{\mu}$ -scheme and μ_0 -scheme in the present section.

A. $\bar{\mu}$ -scheme ($n = -1/2$)

In the $\bar{\mu}$ -scheme, as is explained in the Appendix A, the $\bar{\mu}$ is expressed as

$$\bar{\mu} = \sqrt{\frac{\Delta}{|p|}}, \quad (21)$$

where $\Delta \equiv 2\sqrt{3}\pi\gamma l_{\text{Pl}}^2$ is the area gap. So $\xi = \sqrt{\Delta}$ and $n = -1/2$.

To solve (20) in the considered scheme we introduce a new dependent variables u in the form

$$|p(t)| = u^{1/3}(t). \quad (22)$$

With use of the variable u the equation (20) takes the form

$$\left(\frac{du}{dt}\right)^2 = 9\Omega_I u(t) - 9\Omega_{III}. \quad (23)$$

and has a solution in the form of a second order polynomial

$$u(t) = \frac{\Omega_{III}}{\Omega_I} + \frac{9}{4}\Omega_I t^2 - \frac{18}{4}\Omega_I C_1 t + \frac{9}{4}\Omega_I C_1^2, \quad (24)$$

where C_1 is a constant of integration. We can choose now $C_1 = 0$, so that the minimum of $u(t)$ occurs for $t = 0$. Going back to the canonical variable p we obtain a bouncing solution

$$p(t) = \text{sgn}(p) \left[\frac{\Omega_{III}}{\Omega_I} + \frac{9}{4}\Omega_I t^2 \right]^{1/3}. \quad (25)$$

The main property of this solutions is that $p(t)$ never reaches zero value for non vanishing p_ϕ . The minimal value of $p(t)$ is given by

$$|p_{\min}| = \gamma l_{\text{Pl}}^2 \left[\frac{8\sqrt{3}}{3} \pi^2 \left(\frac{p_\phi}{l_{\text{Pl}}} \right)^2 \right]^{1/3}. \quad (26)$$

We show the solution (25) in the Fig. 1. The dynamical

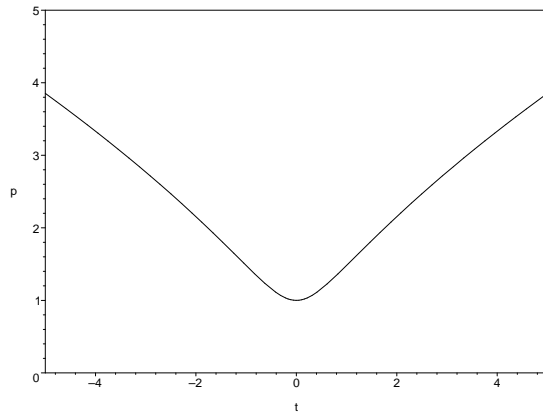


FIG. 1: Typical solution with $\Lambda = 0$ in the $\bar{\mu}$ -scheme. The canonical variable p is expressed in the $[l_{\text{Pl}}^2]$ units and time t in the $[l_{\text{Pl}}]$ units.

behaviour in this model is simple. For negative times we have a contracting pre-Big Bang Universe. For $t > 0$ we have a Big Bang evolution from minimal p_{\min} (26). It is, however, convenient to call this kind of stage Big Bounce rather than Big Bang because of initial singularity avoidance.

B. μ_0 -Scheme ($n = 0$)

In the μ_0 -Scheme the $\bar{\mu}$ is expressed as

$$\bar{\mu} = \mu_0 = \frac{3\sqrt{3}}{2}. \quad (27)$$

So $\xi = \mu_0$ and $n = 0$. To solve (20) in this scheme, we change the time

$$dt = \sqrt{|p(u)|} du \quad (28)$$

and introduce a new variable y as follows

$$y(u) = |p(u)|^2. \quad (29)$$

Applying this new parametrisation to the equation (20) leads to the equation in the form

$$\left(\frac{dy}{du}\right)^2 = 4\Omega_I y(u) - 4\Omega_{III} \quad (30)$$

which has a solution

$$y(u) = \frac{\Omega_{\text{III}}}{\Omega_{\text{I}}} + \Omega_{\text{I}}u^2 - 2\Omega_{\text{I}}C_1u + \Omega_{\text{I}}C_1^2. \quad (31)$$

We can now choose $C_1 = 0$ so that the minimal value of $y(u)$ occurs for $u = 0$. Now we can go back to the initial parameters p and t , then

$$p(u) = \text{sgn}(p)\sqrt{\frac{\Omega_{\text{III}}}{\Omega_{\text{I}}} + \Omega_{\text{I}}u^2} \quad (32)$$

$$t(u) = \int_0^u du' \left[\frac{\Omega_{\text{III}}}{\Omega_{\text{I}}} + \Omega_{\text{I}}u'^2 \right]^{1/4} \quad (33)$$

Introducing the variable

$$x = \frac{\Omega_{\text{I}}}{\sqrt{\Omega_{\text{III}}}}u, \quad (34)$$

we can rewrite integral (33) to the simplest form

$$t(u) = \frac{\sqrt{\Omega_{\text{III}}}}{\Omega_{\text{I}}} \left(\frac{\Omega_{\text{III}}}{\Omega_{\text{I}}} \right)^{1/4} \int_0^{\frac{\Omega_{\text{I}}}{\sqrt{\Omega_{\text{III}}}}u} dx [1 + x^2]^{1/4} \quad (35)$$

and the solution of such integral is given by

$$\int_0^x [1 + y^2]^{1/4} dy = \frac{2}{3}x(1 + x^2)^{1/4} + \frac{1}{3}x {}_2F_1 \left[\frac{1}{2}, \frac{3}{4}, \frac{3}{2}; -x^2 \right], \quad (36)$$

where ${}_2F_1$ is the hypergeometric function, defined as

$${}_pF_q[a_1, \dots, a_p; b_1, \dots, b_q; x] = \sum_{k=0}^{\infty} \frac{(a_1)_k \dots (a_p)_k}{(b_1)_k \dots (b_q)_k} \frac{x^k}{k!}, \quad (37)$$

where $(a)_k$ is the Pochhammer symbol defined as follow

$$(a)_k \equiv \frac{\Gamma(a+k)}{\Gamma(a)} = a(a+1)\dots(a+k-1). \quad (38)$$

This solution is very similar to the one in $\bar{\mu}$ -scheme. However, the time parametrisation is expressed in a more complex way. We show this solution in the Fig. 2. In this case minimal value of $p(t)$ is expressed as

$$|p_{\min}| = \frac{3}{2}\gamma l_{\text{Pl}}^2 \sqrt{\frac{\pi}{2} \left(\frac{p_\phi}{l_{\text{Pl}}} \right)^2}. \quad (39)$$

III. MODELS WITH $\Lambda \neq 0$

In this section, we investigate the general model with non vanishing cosmological constant. It will be useful to write equation (9) in the form

$$\left(\frac{dp}{dt} \right)^2 = \left[\Omega_{\text{I}}|p|^{-1} + \Omega_{\text{II}}|p|^2 \right] \times \left[1 - \frac{\Omega_{\text{III}}}{\Omega_{\text{I}}}|p|^{2n-2} - \frac{\Omega_{\text{V}}}{\Omega_{\text{II}}}|p|^{2n+1} \right]. \quad (40)$$

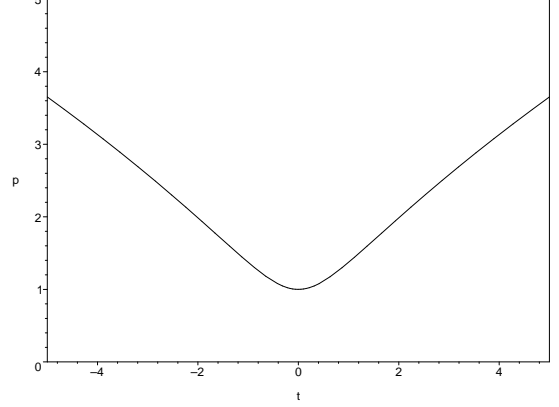


FIG. 2: Typical solution with $\Lambda = 0$ in the μ_0 -scheme. The canonical variable p is expressed in $[l_{\text{Pl}}^2]$ units and time t in the $[l_{\text{Pl}}]$ units.

We see that when we perform the multiplication in this equation and define

$$\Omega_{\text{IV}} = \frac{\Omega_{\text{II}}\Omega_{\text{III}}}{\Omega_{\text{I}}} + \frac{\Omega_{\text{I}}\Omega_{\text{V}}}{\Omega_{\text{II}}}, \quad (41)$$

we recover equation (9). In this and the next section we use equivalently $\Lambda_0 = \frac{3}{\xi^2\gamma^2}$ and $\alpha = \frac{\kappa}{6}p_\phi^2$ to simplify notation.

A. $\bar{\mu}$ -scheme ($n = -1/2$)

In this case equation (40) can be rewritten to the form

$$\left(\frac{dp}{dt} \right)^2 = \gamma_{\text{I}}|p|^2 + \gamma_{\text{II}}|p|^{-1} - \gamma_{\text{III}}|p|^{-4}, \quad (42)$$

where the parameters are defined as

$$\gamma_{\text{I}} = \Omega_{\text{II}} - \Omega_{\text{V}} = \frac{4}{3}\Lambda \left[1 - \frac{\Lambda}{3}\gamma^2\xi^2 \right], \quad (43)$$

$$\gamma_{\text{II}} = \Omega_{\text{I}} - \Omega_{\text{IV}} = \frac{2}{3}\kappa p_\phi^2 \left[1 - 2\frac{\Lambda}{3}\gamma^2\xi^2 \right], \quad (44)$$

$$\gamma_{\text{III}} = \Omega_{\text{III}} = \frac{1}{9}\kappa^2\gamma^2\xi^2 p_\phi^4. \quad (45)$$

To solve equation (42) we re-parametrise the time variable

$$dt = |p(u)|^3 du, \quad (46)$$

and introduce a new variable p as follows

$$y(u) = |p(u)|^3. \quad (47)$$

This change of variables leads to the equation in the form

$$\left(\frac{dy}{du} \right)^2 = 9\gamma_{\text{I}}y^2(y - y_1)(y - y_2), \quad (48)$$

where

$$y_1 = \frac{1}{6} \frac{\kappa p_\phi^2 \gamma^2 \xi^2}{\left[1 - \frac{\Lambda}{3} \gamma^2 \xi^2\right]}, \quad (49)$$

$$y_2 = -\frac{1}{2} \frac{\kappa p_\phi^2}{\Lambda}. \quad (50)$$

There are three general types of solutions corresponding to the values of the parameters (γ_1, y_1, y_2) . We summarise these possibilities in the table below.

	1	2	3
Λ	< 0	> 0	> 0
$1 - \frac{\Lambda}{3} \gamma^2 \xi^2$	> 0	> 0	< 0
γ_1	< 0	> 0	< 0
y_1	> 0	> 0	< 0
y_2	> 0	< 0	< 0

It is important to notice that the product $\Upsilon \equiv \gamma_1 \cdot y_1 \cdot y_2 = -12 \frac{\alpha^2}{\Lambda_0}$ is negative in all cases. This property will be useful to solve equation (48). In the Fig. 3 we show values of the roots y_1 and y_2 as functions of Λ . Thus,

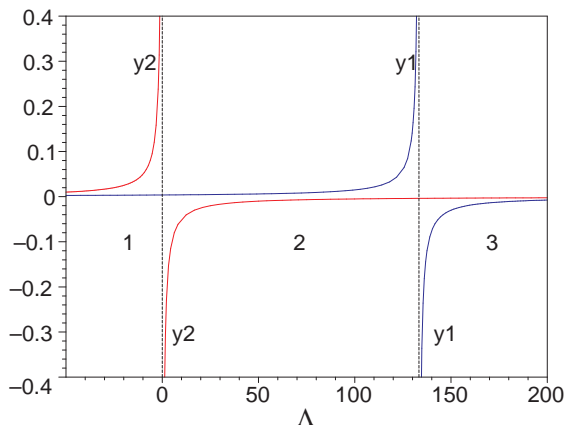


FIG. 3: Parameters y_1 and y_2 as functions of Λ . Region 1 corresponds to oscillatory solution, region 2 to bouncing solution. There is no physical solutions in region 3. The parameter Λ is expressed in units of $[m_{\text{Pl}}^2]$.

there are two values of cosmological constants where the signs of the roots change, namely $\Lambda = 0$ and

$$\Lambda_{0,\bar{\mu}} = \frac{\sqrt{3} m_{\text{Pl}}^2}{2\pi\gamma^3} = 133.4 m_{\text{Pl}}^2, \quad (51)$$

where we have used the value of the $\gamma = \ln 2 / (\pi\sqrt{3})$ calculated in the work [18]. More recent investigation of the black hole entropy indicate however that the value of the Barbero-Immirzi parameter is $\ln 2/\pi \leq \gamma \leq \ln 3/\pi$ [19]. In particular, Meissner has calculated $\gamma_M = 0.12738$ [20]. However, this freedom in the choice of γ does not change the qualitative results. Only the region of the

parameter space where the particular kind of motion is allowed can be shifted.

We now perform a change of variables in equation (48) in the form

$$w(u) = \frac{1}{y(u)}, \quad (52)$$

and

$$\chi = 3\sqrt{|\Upsilon|}u. \quad (53)$$

We also introduce the parameters

$$w_1 = \frac{1}{y_1}, \quad w_2 = \frac{1}{y_2}, \quad (54)$$

and then equation (48) takes the form

$$\left(\frac{dw}{d\chi}\right)^2 = -(w_1 - w)(w_2 - w). \quad (55)$$

The equation (55) is the equation of shifted harmonic oscillator and its solution is

$$w(\chi) = \frac{\Lambda_{0,\bar{\mu}}}{6\alpha} \left[1 - 2\frac{\Lambda}{\Lambda_{0,\bar{\mu}}} + \cos(\chi) \right]. \quad (56)$$

where we set the integration constant to zero. It is now possible to go back to the initial parameters p and t which are expressed as follows

$$p(u) = \text{sgn}(p) \frac{\sqrt[3]{\frac{6\alpha}{\Lambda_{0,\bar{\mu}}}}}{\sqrt[3]{1 - 2\frac{\Lambda}{\Lambda_{0,\bar{\mu}}} + \cos\left(3\sqrt{|\Upsilon|}u\right)}}, \quad (57)$$

$$t(u) = \int_0^u du' p^3(u'), \quad (58)$$

The integral (58) can be easily solved but solutions depend on the parameters in (57).

We define now an integral

$$I(x, a) = \int_0^x \frac{dx'}{a + \cos x'} \quad (59)$$

so the expression (58) can now be written as

$$t(u) = \frac{1}{3\sqrt{|\Upsilon|}} I\left(3\sqrt{|\Upsilon|}u, 1 - 2\frac{\Lambda}{\Lambda_{0,\bar{\mu}}}\right) \quad (60)$$

Solutions of integral (59) depend on the value of parameter a and read

$$I(x, |a| > 1) = \frac{2}{\sqrt{a^2 - 1}} \arctan \left[\frac{(a - 1) \tan\left(\frac{x}{2}\right)}{\sqrt{a^2 - 1}} \right],$$

$$I(x, a = 1) = \tan\left(\frac{x}{2}\right),$$

$$I(x, 0 < |a| < 1) = -\frac{2}{\sqrt{1 - a^2}} \operatorname{arctanh} \left[\frac{(a - 1) \tan\left(\frac{x}{2}\right)}{\sqrt{1 - a^2}} \right],$$

$$I(x, a = 0) = \ln \left(\frac{1}{\cos x} - \tan x \right).$$

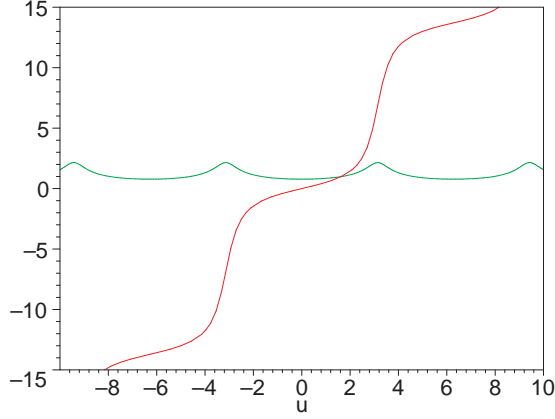


FIG. 4: Parametric solution with $\Lambda < 0$. Oscillating curve (green) is $|p(u)|$ and the increasing curve (red) is $t(u)$. The canonical variable p is expressed in the $[l_{P1}^2]$ units and time t in the $[l_{P1}]$ units.

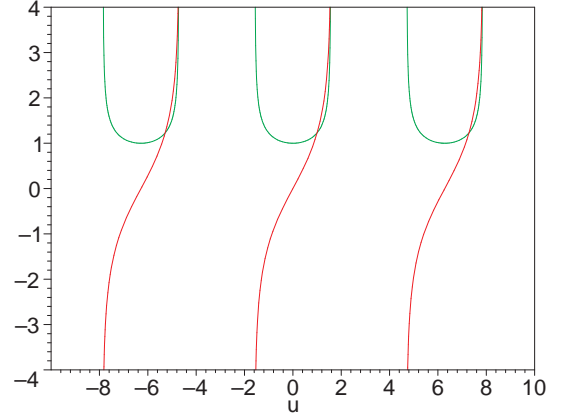


FIG. 6: Parametric solution with $0 < \Lambda < \Lambda_{0, \bar{\mu}}$. Top curve (green) shows $|p(u)|$ and bottom curve (red) is $t(u)$. The canonical variable p is expressed in units of $[l_{P1}^2]$ and time t in $[l_{P1}]$.

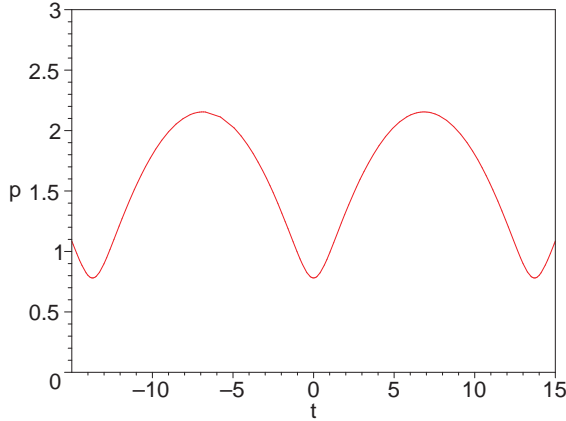


FIG. 5: Solution $|p(t)|$ with $\Lambda < 0$. The canonical variable p is expressed in units of $[l_{P1}^2]$ and time t in $[l_{P1}]$.

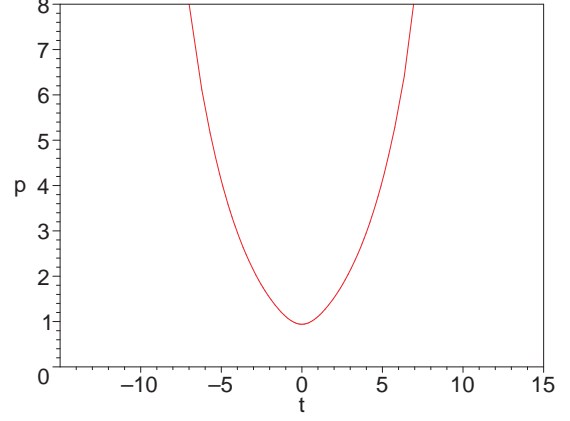


FIG. 7: Solution $|p(t)|$ with $0 < \Lambda < \Lambda_{0, \bar{\mu}}$. The canonical variable p is expressed in units of $[l_{P1}^2]$ and time t in $[l_{P1}]$.

In Fig. 4 we show the solution for $\Lambda < 0$ – or equivalently with parameter $a > 1$.

In Fig. 5 we show the solution for $0 < \Lambda < \Lambda_{0, \bar{\mu}}$ which corresponds to $0 < |a| < 1$.

B. μ_0 -Scheme ($n = 0$)

In this section we study the last case in which $n = 0$ and $\xi = 3\sqrt{3}/2$. Equation (40) can then be written in the form

$$\left(\frac{dp}{dt}\right)^2 = |p|^{-3} \left(\Omega_I + \Omega_{II}|p|^3\right) W(|p|), \quad (61)$$

where

$$W(|p|) = |p|^3 a_3 + |p|^2 a_2 + |p| a_1 + a_0, \quad (62)$$

and the polynomial's coefficients are expressed as

$$a_0 = -\frac{1}{6} \kappa p_\phi^2 \gamma^2 \xi^2 = -\frac{3\alpha}{\Lambda_{0, \mu_0}}, \quad (63)$$

$$a_1 = 0, \quad (64)$$

$$a_2 = 1, \quad (65)$$

$$a_3 = -\frac{\Lambda}{3} \gamma^2 \xi^2 = -\frac{\Lambda}{\Lambda_{0, \mu_0}}. \quad (66)$$

The discriminant of polynomial (62) is

$$\tilde{\Delta} = \frac{a_2^2 a_1^2 - 4a_1^3 a_3 - 4a_2^3 a_0 + 18a_0 a_1 a_2 a_3 - 27a_0^2 a_3^2}{a_3^4}. \quad (67)$$

Inserting the values of parameters $\{a_0, a_1, a_2, a_3\}$ listed above we obtain

$$\tilde{\Delta} = \left(\frac{\Lambda}{\Lambda_{0, \mu_0}}\right)^{-4} \left[\frac{12\alpha}{\Lambda_{0, \mu_0}} - 27 \left(\frac{3\alpha}{\Lambda_{0, \mu_0}} \frac{\Lambda}{\Lambda_{0, \mu_0}}\right)^2 \right]. \quad (68)$$

For $\tilde{\Delta} > 0$, or

$$\frac{4}{81} > \left(\frac{\alpha}{\Lambda_{0,\mu_0}}\right) \left(\frac{\Lambda}{\Lambda_{0,\mu_0}}\right)^2 \quad (69)$$

polynomial (62) has three real roots. When relation (69) is fulfilled and $\Lambda > 0$, oscillatory solutions occur. For $\Lambda < 0$ equation (61) has bouncing type solutions. This can be seen when we redefine equation (61) to the point particle form. This approach is useful for qualitative analysis and will be fully used in the next section. However, here we will use it to distinguish between different types of solutions.

Introducing a new time variable

$$dt = \frac{|p|^{3/2}}{\sqrt{\Omega_I + \Omega_{II}|p|^3}} du, \quad (70)$$

we can rewrite equation (61) to the form

$$\mathcal{H} = \frac{1}{2}p'^2 + V(p) = E = -\frac{3}{2} \frac{\alpha}{\Lambda_{0,\mu_0}}, \quad (71)$$

where the potential function

$$V(p) = -\frac{1}{2}|p|^2 \left(1 - \frac{\Lambda}{\Lambda_{0,\mu_0}}|p|\right). \quad (72)$$

Equation (71) has the form of Hamiltonian constraint for a point particle in a potential well. We see that for $\Lambda < 0$ potential (72) has only one extremum (for $p = 0$) and only a bouncing solution is possible. For $\Lambda > 0$ potential (72) has a minimum for $|p_{\min}| = \frac{2}{3} \frac{\Lambda_{0,\mu_0}}{\Lambda}$. In this case physical solutions correspond to the condition $E > V(|p_{\min}|)$ and the energy of the imagined particle in the potential well is greater than the minimum of well. The particle then oscillates between the boundaries of the potential. The condition $E > V(|p_{\min}|)$ is equivalent to relation (69) calculated from the discriminant.

Upon introducing the parameters

$$g_2 := \frac{1}{12}a_2^2 - \frac{1}{4}a_3a_1, \quad (73)$$

$$g_3 := \frac{1}{48}a_3a_2a_1 - \frac{1}{216}a_2^3 - \frac{1}{16}a_3^2a_0, \quad (74)$$

and the variable v

$$|p| = \frac{4}{a_3}v - \frac{a_2}{3a_3} \quad (75)$$

then equation (61) takes on the form of the Weierstrass equation

$$\left(\frac{dv}{du}\right)^2 = 4v^3 - g_2v - g_3. \quad (76)$$

Detailed analysis and plots of solutions of this equation for different values of parameters can be found in the

appendix to the article [17]. The solution of equation (76) is the Weierstrass \wp -function

$$v(u) = \wp(u - u_0; g_2, g_3), \quad (77)$$

where

$$g_2 = \frac{1}{12}, \quad (78)$$

$$g_3 = -\frac{1}{216} + \frac{1}{16} \left(\frac{\Lambda}{\Lambda_{0,\mu_0}}\right)^2 \frac{3\alpha}{\Lambda_{0,\mu_0}}. \quad (79)$$

So the parametric solution for the parameter p is

$$p(u) = \text{sgn}(p) \frac{\Lambda_{0,\mu_0}}{\Lambda} \left[\frac{1}{3} - 4\wp(u - u_0; g_2, g_3) \right] \quad (80)$$

The time variable can be expressed as the integral

$$t(u) = \int_0^u du' \frac{\left(\frac{4}{a_3}v(u') - \frac{a_2}{3a_3}\right)^{3/2}}{\sqrt{\Omega_I + \Omega_{II} \left(\frac{4}{a_3}v(u') - \frac{a_2}{3a_3}\right)^3}}. \quad (81)$$

In the Fig. 8 and 9 we show an exemplary parametric bounce solution with $\Lambda < 0$ and a possible oscillatory solution with $\Lambda > 0$.

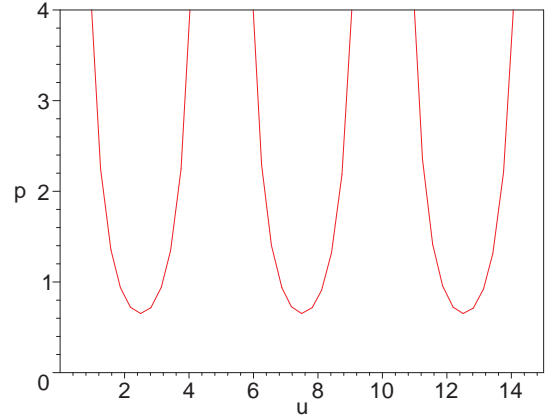


FIG. 8: Parametric solution $|p(u)|$ with $\Lambda < 0$. The canonical variable p is expressed in units of $[l_{\text{Pl}}^2]$, u is dimensionless.

In general the solution is expressible as an explicit function of time, by means of the so called Abelian functions. However, we chose not to employ them here as the appropriate formulae are not as clear, and the commonly used numerical packages do not allow for their direct plotting. The fact of existence of such solutions allows us to assume that the above integral is well defined, and so is the solution itself.

IV. QUALITATIVE METHODS OF DIFFERENTIAL EQUATIONS IN STUDY EVOLUTIONAL PATHS

The main advantage of using qualitative methods of differential equations (dynamical systems methods) is the

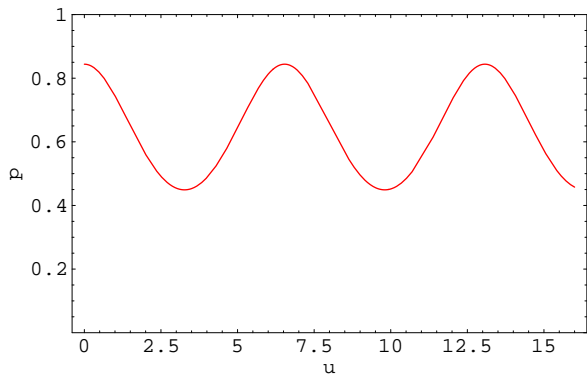


FIG. 9: Parametric solution $|p(u)|$ with $\Lambda > 0$ and relation (69) satisfied. The canonical variable p is expressed in units of $[l_{\text{P}}^2]$ and u is dimensionless.

investigation of all solutions for all admissible initial conditions. We demonstrate that dynamics of the model can be reduced to the form of two dimensional autonomous dynamical system. In our case the phase space is $2D$ (p, \dot{p}) . First we can find the solutions corresponding to vanishing of the right hand sides of the system which are called critical points. The information about their stability and character is contained in the linearisation matrix around a given critical point. In the considered case, the dynamical system is of the Newtonian type. For such a system, the characteristic equation which determines the eigenvalues of the linearisation matrix at the critical point is of the form $\lambda^2 + \partial^2 V(p)/\partial p^2$ where $V(p)$ is a potential function and $|p| = a^2 V_0^{2/3}$, a being the scale factor. As it is well known for dynamical systems of the Newtonian type, only two types of critical points are admissible. If the diagram of the potential function is upper convex then eigenvalues are real and of opposite signs, and the corresponding critical point is of the saddle type. In the opposite case, if $\partial^2 V(p)/\partial p^2 > 0$ then the eigenvalues are purely imaginary and conjugate. The corresponding critical point is of the centre type.

Equation (40) can be written in the form

$$\frac{1}{4}\dot{p}^2 = |p|^{2n-3} \left(\alpha + \frac{\Lambda}{3}|p|^3 \right) \left(|p|^{-2n+2} - \gamma^2 \xi^2 \left(\alpha + \frac{\Lambda}{3}|p|^3 \right) \right), \quad (82)$$

where $\alpha = \frac{\kappa}{6} p_\phi^2$ or equivalently as

$$\frac{1}{4} \frac{|p|^{-2n+3}}{\alpha + \frac{\Lambda}{3}|p|^3} \dot{p}^2 = p'^2 = |p|^2 \left(|p|^{-2n} - \gamma^2 \xi^2 \frac{\Lambda}{3} |p| \right) - \gamma^2 \xi^2 \alpha, \quad (83)$$

where we have made the following time reparametrisation $t \rightarrow u$

$$\frac{d}{du} = \frac{1}{2} \frac{|p|^{-n+3/2}}{\sqrt{\alpha + \frac{\Lambda}{3}|p|^3}} \frac{d}{dt}. \quad (84)$$

Now we are able to write the Hamiltonian constraint in the form analogous to the particle of the unit mass

moving in the one dimensional potential well

$$\mathcal{H} = \frac{1}{2} p'^2 + V(p) = E = -\gamma^2 \xi^2 \frac{\alpha}{2}, \quad (85)$$

where the potential function

$$V(p) = -\frac{1}{2} |p|^2 \left(|p|^{-2n} - \gamma^2 \xi^2 \frac{\Lambda}{3} |p| \right). \quad (86)$$

As we can see, the constant $-\gamma^2 \xi^2 \alpha/2$ plays the role of the total energy of the fictitious particle. The domain admissible for motion in the configuration space is determined by the condition $V(p) + \gamma^2 \xi^2 \alpha/2 < 0$.

A dynamical system of the Hamiltonian type has the following form

$$\begin{aligned} p' &= y, \\ y' &= -\frac{\partial V}{\partial p}, \end{aligned} \quad (87)$$

where the prime denotes differentiation with respect to a new re-parametrised time variable which is a monotonous function of the original, cosmological time.

The structure of the phase plane is organised by the number and location of critical points. In our case, critical points in the finite domain are located only on the line $p' = y = 0$ and the second coordinate is determined from the equation $-\partial V/\partial p = 0$ which is

$$p \left((1-n)|p|^{-2n} - \gamma^2 \xi^2 \frac{\Lambda}{2} |p| \right) = 0. \quad (88)$$

The number of critical points depends on the value of Λ and n . We can distinguish two cases:

- for $-1/2 < n \leq 0$:
 - $\Lambda < 0$: $(|p|, p') = (0, 0)$;
 - $\Lambda > 0$: $(|p|, p') = (0, 0)$ and $(|p|, p') = \left(\sqrt[2n+1]{\frac{2(1-n)}{\gamma^2 \xi^2 \Lambda}}, 0 \right)$;
- for $n = -1/2$:
 - $\Lambda \neq \frac{3}{\gamma^2 \xi^2}$: $(|p|, p') = (0, 0)$;
 - $\Lambda = \frac{3}{\gamma^2 \xi^2}$: degenerate $V(p) = 0$.

The full analysis of the behaviour of trajectories requires investigation also at the infinity. To this aim we introduce radial coordinates on the phase plane for compactification of the plane by adjoining the circle at infinity $p = \frac{r}{1-r} \cos \theta$, $y = \frac{r}{1-r} \sin \theta$.

The phase portraits for both cases are shown at Figs. 10 and 11.

For the general case of $\Lambda > 0$ we can write the parametric equation of the boundary $\alpha = 0$ of the physically admissible region in the phase space, namely

$$p^2 = \frac{4}{3} \Lambda |p|^2 \left(1 - \gamma^2 \xi^2 \frac{\Lambda}{3} |p|^{2n+1} \right), \quad (89)$$

where the dot denotes differentiation with respect to cosmological time t . This equation greatly simplifies for the

special case $n = -1/2$, and we receive the value of the Hubble parameter at the boundary

$$\frac{1}{4} \frac{\dot{p}^2}{|p|^2} = H^2 = \frac{\Lambda}{3} (1 - \gamma^2 \xi^2 \frac{\Lambda}{3}). \quad (90)$$

In this special case $\alpha = 0$ and $n = 0$ we can integrate eq.(1) for $\Lambda > 0$ and choosing the integration constant equal to zero

$$p(t) = \text{sgn}(p) \frac{\Lambda_{0,\mu_0}}{\Lambda} \frac{1}{\cosh^2\left(\sqrt{\frac{\Lambda}{3}}t\right)}, \quad (91)$$

which gives the maximal value of parameter p

$$|p_{\max}| = \frac{\Lambda_0}{\Lambda}. \quad (92)$$

In the same case with $\Lambda < 0$ and choosing integration constant equal to zero we have

$$p(t) = \text{sgn}(p) \frac{\Lambda_{0,\mu_0}}{\Lambda} \frac{1}{\sinh^2\left(\sqrt{\frac{\Lambda}{3}}t\right)}. \quad (93)$$

For $\alpha = 0$ and $\Lambda < \Lambda_{0,\bar{\mu}}$ in the case $n = -1/2$ we obtain the de Sitter solution

$$p(t) = \text{sgn}(p) \text{const} \cdot \exp\left\{2\sqrt{1 - \frac{\Lambda}{\Lambda_{0,\bar{\mu}}}}\sqrt{\frac{\Lambda}{3}}t\right\}. \quad (94)$$

These solutions represent the lines on the boundaries of the physically admissible domains.

V. SUMMARY

We have studied dynamics and analytical solutions of the flat Friedmann-Robertson-Walker cosmological model with a free scalar field and the cosmological constant, modified by the holonomy corrections of Loop Quantum Gravity.

We performed calculations in two setups called $\bar{\mu}$ -scheme and μ_0 -scheme, explained in the appendix A. We have explored whole $\Lambda \in \mathbb{R}$ range and whole allowed $p_\phi^2 \in \mathbb{R}_+ \cup \{0\}$ range. In the case of $\bar{\mu}$ -scheme resulting solutions are of oscillating type for $\Lambda \in \mathbb{R}_-$ and bouncing type for $\Lambda \in (0, \Lambda_0)$. For $\Lambda \in [\Lambda_0, \infty)$ there are no physical solutions. In the case of μ_0 -scheme for $\Lambda \in \mathbb{R}_-$ bouncing solutions occur. When both $\Lambda \in \mathbb{R}_+$ and relation (69) are fulfilled, oscillatory behaviour occurs. Otherwise, bouncing solutions appear. In all considered cases with $p_\phi^2 \in \mathbb{R}_+$ the initial singularity is avoided.

We have investigated the evolutionary paths of the model, from the point of view of qualitative methods of dynamical systems of differential equations. We found that in the special case of $n = -1/2$ the boundary trajectory ($\alpha = 0$) approaches the de Sitter state; and demonstrate that in the case of positive cosmological constant

there are two types of dynamical behaviours in the finite domain. For the case of $n = 0$ there appear oscillating solutions without the initial and final singularities, and that they change into bouncing for $0 > n \geq -1/2$.

The results of this paper can give helpful background dynamics to study variety of physical phenomenas during the bounce epoch in Loop Quantum Cosmology. For example, the interesting question of the fluctuations like gravitational waves[21, 22, 23] or scalar perturbations [24] during this period. We tried to show that numerical calculations can be “shifted” one step further, since the basic model is explicitly solvable, and can be treated as starting ground for more complex problems, like the above, which cannot be solved analytically.

Acknowledgments

Authors are grateful to Orest Hrycyna for discussion. This work was supported in part by the Marie Curie Actions Transfer of Knowledge project COCOS (contract MTKD-CT-2004-517186).

APPENDIX A: FLAT FRW MODEL AND HOLONOMY CORRECTIONS IN LOOP QUANTUM GRAVITY

In this appendix, we derive the form of the Hamiltonian (1) considered in the paper.

The FRW $k = 0$ spacetime metric can be written as

$$ds^2 = -N^2(x)dt^2 + q_{ab}dx^a dx^b, \quad (A1)$$

where $N(x)$ is the lapse function and the spatial part of the metric is expressed as

$$q_{ab} = \delta_{ij}\omega_a^i\omega_b^j = a^2(t) {}^o q_{ab} = a^2(t)\delta_{ij} {}^o\omega_a^i {}^o\omega_b^j. \quad (A2)$$

In this expression ${}^o q_{ab}$ is fiducial metric and ${}^o\omega_a^i$ are cotriads dual to the triads ${}^o e_i^a$, ${}^o\omega^i({}^o e_j) = \delta_j^i$ where ${}^o\omega^i = {}^o\omega_a^i dx^a$ and ${}^o e_i = {}^o e_i^a \partial_a$. From these triads we construct the Ashtekar variables

$$A_a^i \equiv \Gamma_a^i + \gamma K_a^i = \tilde{c} {}^o\omega_a^i, \quad (A3)$$

$$E_i^a \equiv \sqrt{|\det q|} e_i^a = \tilde{p} \sqrt{{}^o q} {}^o e_i^a, \quad (A4)$$

where

$$|\tilde{p}| = a^2, \quad (A5)$$

$$\tilde{c} = \gamma \dot{a}. \quad (A6)$$

Note that the Gaussian constraint implies that $\tilde{p} \leftrightarrow -\tilde{p}$ leads to the same physical results. The factor γ is called Barbero-Immirzi parameter. In the definition (A3) the spin connection is defined as

$$\Gamma_a^i = -\epsilon^{ijk} e_j^b (\partial_{[a} e_{b]}^k + \frac{1}{2} e_k^c e_a^l \partial_{[c} e_{b]}^l), \quad (A7)$$

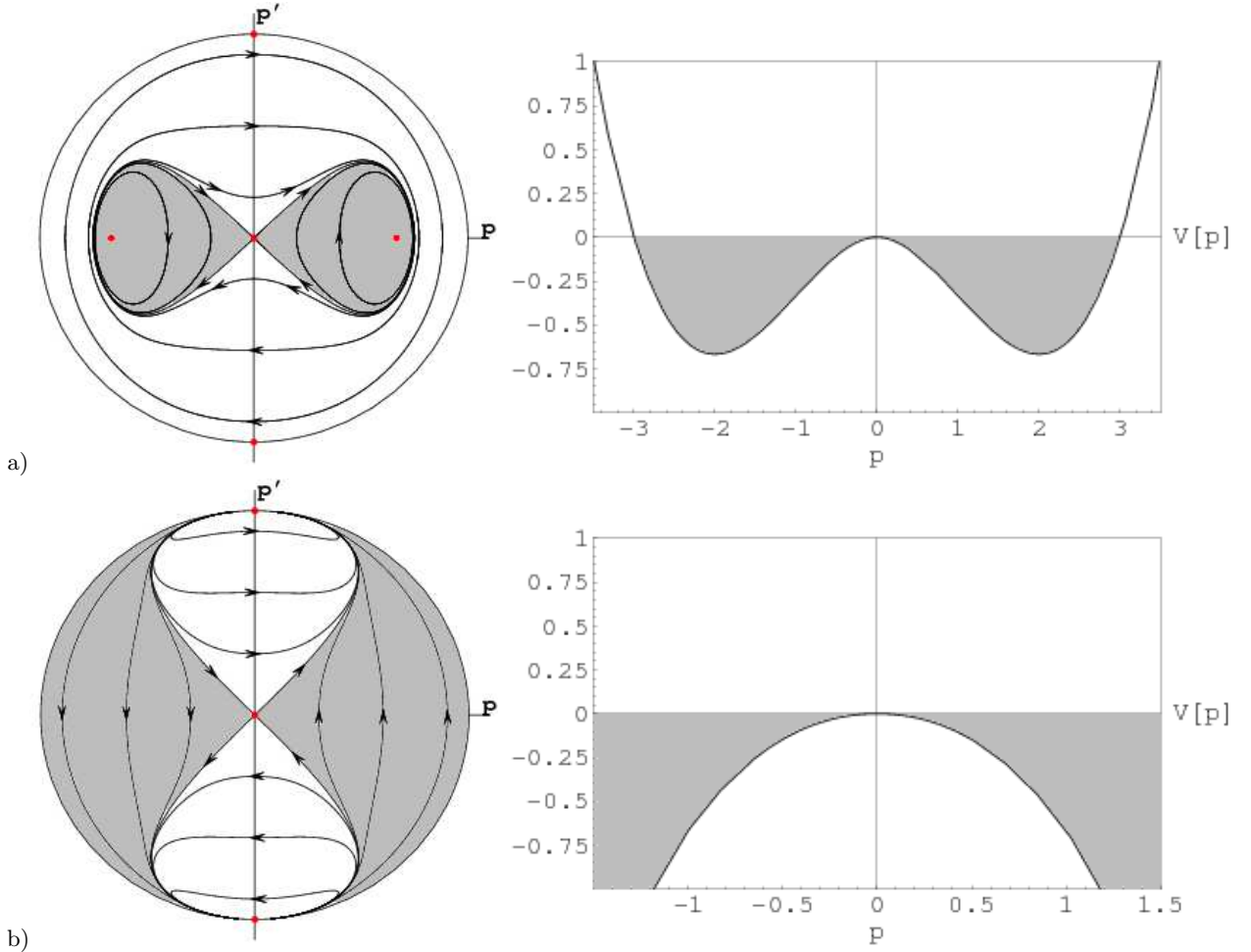


FIG. 10: The phase space diagram for the case $n = 0$ and a) $\Lambda > 0$ and b) $\Lambda < 0$. The physical domain admissible for motion is shaded. Note that for the case (a) the boundary of admissible for motion is bounded by a homoclinic orbit and all solutions in this area are oscillating without initial and final singularities. All trajectories situated in physical region posses the minimum value of scale factor.

and the extrinsic curvature is defined as

$$K_{ab} = \frac{1}{2N} [\dot{q}_{ab} - 2D_{(a}N_{b)}], \quad (\text{A8})$$

which corresponds to $K_a^i := K_{ab}e_i^b$.

The scalar constraint, in Ashtekar variables, has the form

$$H_G = \frac{1}{16\pi G} \int_{\Sigma} d^3x N(x) \frac{E_i^a E_j^b}{\sqrt{|\det E|}} [\varepsilon^{ij}{}_k F_{ab}^k - 2(1 + \gamma^2) K_{[a}^i K_{b]}^j], \quad (\text{A9})$$

where field strength is expressed as

$$F_{ab}^k = \partial_a A_b^k - \partial_b A_a^k + \varepsilon_{ij}^k A_a^i A_b^j. \quad (\text{A10})$$

With use of (A3),(A4) and (A10) the Hamiltonian (A9) assumes the form

$$H_G = -\frac{3V_0}{8\pi G \gamma^2} \sqrt{|\tilde{p}|} \tilde{c}^2, \quad (\text{A11})$$

where we have assumed a gauge of $N(x) = 1$. The constant V_0 is the volume of the fiducial cell. This volume can be chosen arbitrarily. It is convenient to absorb the factor V_0 by redefinition

$$p = \tilde{p}V_0^{2/3}, \quad c = \tilde{c}V_0^{1/3}. \quad (\text{A12})$$

The holonomy along a curve $\alpha \in \Sigma$ is defined as follows

$$h_{\alpha} = \mathcal{P} \exp \int_{\alpha} \tau_i A_a^i dx^a, \quad (\text{A13})$$

where $2i\tau_i = \sigma_i$ and σ_i are the Pauli matrices. From this definition we can calculate holonomy in the direction ${}^{\circ}e_i^a \partial_a$ and the length $\mu V_0^{1/3}$

$$\begin{aligned} h_i^{(\mu)} &= \exp \int_0^{\mu V_0^{1/3}} \tau_i c V_0^{-1/3} \omega_a^i dx^a = \exp \tau_i \mu c \\ &= \mathbb{I} \cos\left(\frac{\mu c}{2}\right) + 2\tau_i \sin\left(\frac{\mu c}{2}\right), \end{aligned} \quad (\text{A14})$$

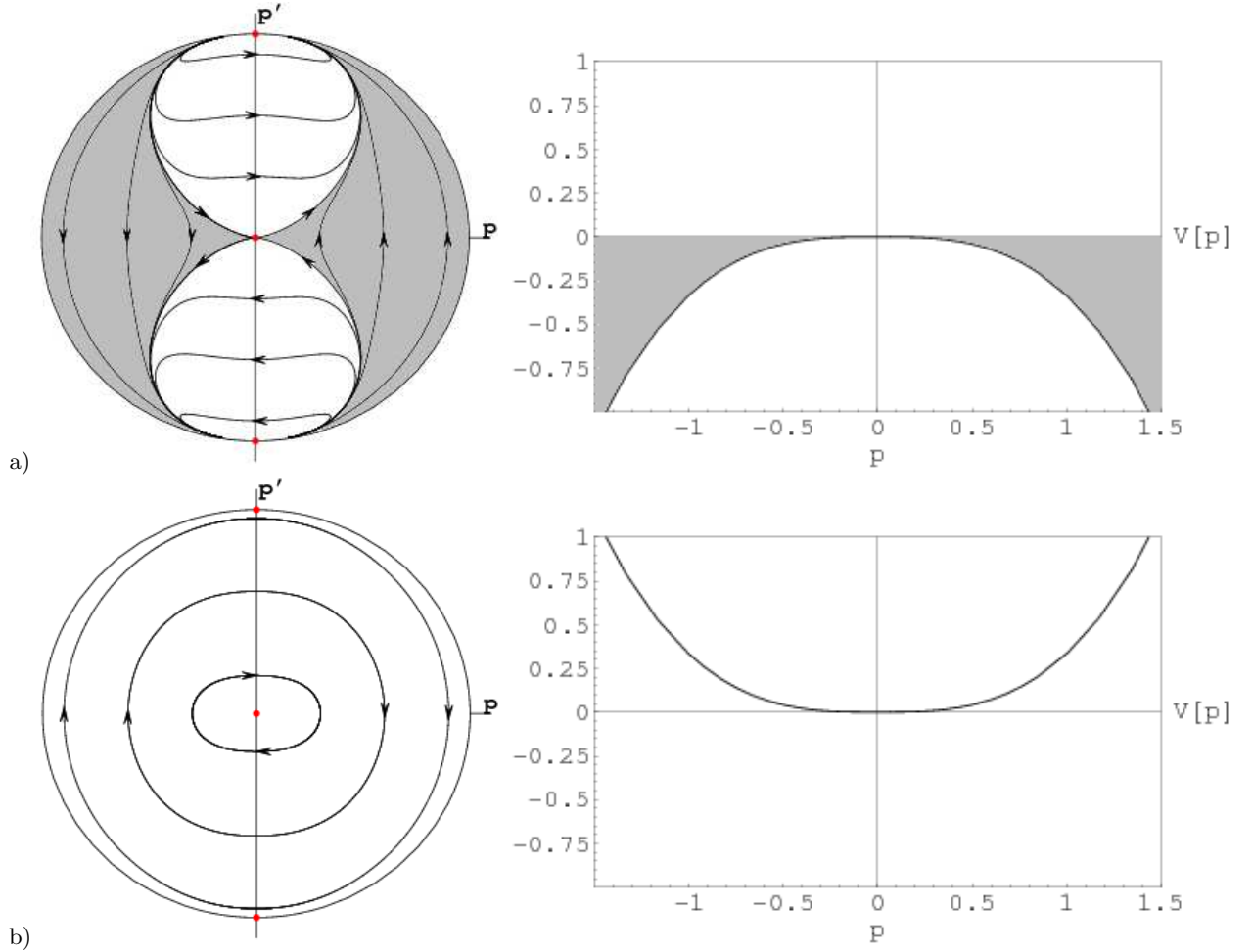
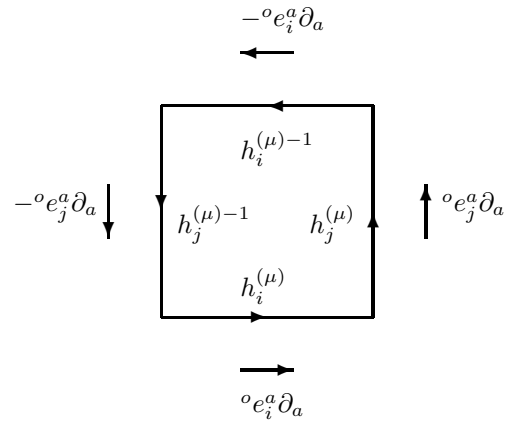


FIG. 11: The phase space diagram for the case $n = -1/2$ and a) $\Lambda = \frac{1}{\gamma^2 \xi^2} < \frac{3}{\gamma^2 \xi^2} = \Lambda_0$ and b) $\Lambda = \frac{5}{\gamma^2 \xi^2} > \frac{3}{\gamma^2 \xi^2} = \Lambda_0$. The physical domain admissible for motion is shaded. In the second case there is no physically allowed region for which $\alpha > 0$. This case is distinguished by behaviour at infinity when Hubble function is finite like for the de Sitter solution (see formula (90)). This state is the global attractor in the future. All solutions are of the bouncing type.

where we used definition of the Ashtekar variable A (A3). From such a particular holonomies we can construct holonomy along the closed curve $\alpha = \square_{ij}$. This curve is schematically presented on the diagram below.



This holonomy can be written as

$$\begin{aligned}
h_{\square_{ij}}^{(\mu)} &= h_i^{(\mu)} h_j^{(\mu)} h_i^{(\mu)-1} h_j^{(\mu)-1} \\
&= e^{\mu V_0^{1/3} A_a \circ e_a^i} e^{\mu V_0^{1/3} A_a \circ e_a^j} e^{-\mu V_0^{1/3} A_a \circ e_a^i} e^{-\mu V_0^{1/3} A_a \circ e_a^j} \\
&= \exp \left[\mu^2 V_0^{2/3} A_a^l A_b^m \circ e_i^{a \circ} e_j^{b \circ} [\tau_l, \tau_m] + \mathcal{O}(\mu^3) \right] \\
&= \mathbb{I} + \mu^2 V_0^{2/3} F_{ab}^k \tau_k \circ e_i^{a \circ} e_j^{b \circ} + \mathcal{O}(\mu^3), \tag{A15}
\end{aligned}$$

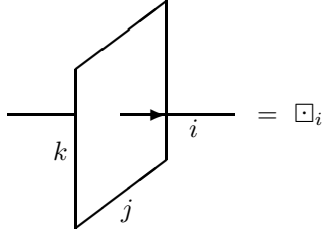
where we have used Baker-Campbell-Hausdorff formula and the fact that for flat FRW, field strength (A10) simplifies to the form $F_{ab}^k = \epsilon_{ij}^k A_a^i A_b^j$. Now, equation (A15) can be simply rewritten to the form

$$F_{ab}^k = -2 \lim_{\mu \rightarrow 0} \frac{\text{tr} \left[\tau_k \left(h_{\square_{ij}}^{(\mu)} - \mathbb{I} \right) \right]}{\mu^2 V_0^{2/3}} \circ \omega_a^i \circ \omega_b^j. \tag{A16}$$

The trace in this equation can be calculated with use of definition (A14)

$$\text{tr} \left[\tau_k \left(h_{\square_{ij}}^{(\mu)} - \mathbb{I} \right) \right] = -\frac{\epsilon_{kij}}{2} \sin^2(\mu c). \tag{A17}$$

In Loop Quantum Gravity the limit $\mu \rightarrow 0$ in the formula (A16) does not exist because of existence of the area gap. The area gap corresponds to the minimal quantum of area $\Delta = 2\sqrt{3}\pi\gamma l_{\text{Pl}}^2$, which arises as the first non-zero eigenvalue of the area operator [26]. So instead of the limit in equation (A16) we should stop shrinking the loop at the appropriate minimal area Δ . This area corresponds to the area intersected by the loop. For the holonomy in the direction $\circ e_i^a \partial_a$ the area is \square_i , as explained in the diagram below (where $i = k \wedge j$).



The limit $\square_i \rightarrow \Delta$ corresponds to $\mu \rightarrow \bar{\mu}$. Now, we must connect the area \square_i with the length μ . We can

choose that area \square_i to correspond to physical area $a^2 \mu^2$ or to the area μ^2 . So in the case $\square_i = V_0^{2/3} a^2 \mu^2 = |p| \mu^2$ we have the limit

$$\mu \rightarrow \bar{\mu} = \sqrt{\frac{\Delta}{|p|}}. \tag{A18}$$

This approach we call $\bar{\mu}$ -scheme. In the case $\square_i = |p_0| \mu^2$ where p_0 correspond to the eigenvalue

$$\hat{p}|\mu_0\rangle = \mu_0 \frac{8\pi\gamma l_{\text{Pl}}^2}{6} |\mu_0\rangle, \tag{A19}$$

and taking the limit

$$\mu \rightarrow \bar{\mu} = \mu_0 = \frac{3\sqrt{3}}{2}, \tag{A20}$$

which we call μ_0 -scheme.

In the quantum version, we can combine equations (A16) and (A17), and write

$$F_{ab}^k = \frac{\sin^2(\bar{\mu}c)}{\bar{\mu}^2 V_0^{2/3}} \epsilon_{kij} \circ \omega_a^i \circ \omega_b^j, \tag{A21}$$

whereas in the classical case we have

$$F_{ab}^k = \frac{c^2}{V_0^{2/3}} \epsilon_{kij} \circ \omega_a^i \circ \omega_b^j. \tag{A22}$$

So, from these two equations we see that quantum effects can be introduced by a replacement

$$c \rightarrow \frac{\sin(\bar{\mu}c)}{\bar{\mu}} \tag{A23}$$

in the classical expressions. The Hamiltonian (A11) with holonomy correction takes the form

$$H_{\text{eff}} = -\frac{3}{8\pi G \gamma^2} \sqrt{|p|} \left[\frac{\sin(\bar{\mu}c)}{\bar{\mu}} \right]^2. \tag{A24}$$

-
- [1] P. Singh, K. Vandersloot and G. V. Vereshchagin, Phys. Rev. D **74** (2006) 043510 [arXiv:gr-qc/0606032].
- [2] A. Ashtekar, T. Pawłowski and P. Singh, Phys. Rev. D **73** (2006) 124038 [arXiv:gr-qc/0604013].
- [3] T. Stachowiak and M. Szydlowski, Phys. Lett. B **646** (2007) 209 [arXiv:gr-qc/0610121].
- [4] A. Ashtekar, T. Pawłowski and P. Singh, Phys. Rev. Lett. **96** (2006) 141301 [arXiv:gr-qc/0602086].
- [5] M. Bojowald, Class. Quant. Grav. **19** (2002) 2717 [arXiv:gr-qc/0202077].
- [6] M. Bojowald, Class. Quant. Grav. **20** (2003) 2595 [arXiv:gr-qc/0303073].
- [7] A. Ashtekar, T. Pawłowski and P. Singh, Phys. Rev. D **74** (2006) 084003 [arXiv:gr-qc/0607039].
- [8] A. Ashtekar, T. Pawłowski, P. Singh and K. Vandersloot, Phys. Rev. D **75** (2007) 024035 [arXiv:gr-qc/0612104].
- [9] M. Bojowald, Phys. Rev. D **74** (2007) 081301 [arXiv:gr-qc/0608100].
- [10] M. Bojowald, arXiv:0801.4001 [gr-qc].
- [11] K. Vandersloot, Phys. Rev. D **75** (2007) 023523 [arXiv:gr-qc/0612070].
- [12] L. Szulc, W. Kaminski and J. Lewandowski, Class. Quant. Grav. **24** (2007) 2621 [arXiv:gr-qc/0612101].
- [13] L. Szulc, arXiv:0707.1816 [gr-qc].

- [14] D. W. Chiou, arXiv:0710.0416 [gr-qc].
- [15] D. W. Chiou, arXiv:gr-qc/0703010.
- [16] M. Bojowald, *Gen. Rel. Grav.* **40**, 639 (2008) [arXiv:0705.4398 [gr-qc]].
- [17] M. P. Dabrowski and T. Stachowiak, *Annals Phys.* **321** (2006) 771 [arXiv:hep-th/0411199].
- [18] A. Ashtekar, J. Baez, A. Corichi and K. Krasnov, *Phys. Rev. Lett.* **80** (1998) 904 [arXiv:gr-qc/9710007].
- [19] M. Domagala and J. Lewandowski, *Class. Quant. Grav.* **21** (2004) 5233 [arXiv:gr-qc/0407051].
- [20] K. A. Meissner, *Class. Quant. Grav.* **21** (2004) 5245 [arXiv:gr-qc/0407052].
- [21] M. Bojowald and G. M. Hossain, arXiv:0709.2365 [gr-qc].
- [22] J. Mielczarek and M. Szydlowski, *Phys. Lett. B* **657** (2007) 20 [arXiv:0705.4449 [gr-qc]].
- [23] J. Mielczarek and M. Szydlowski, arXiv:0710.2742 [gr-qc].
- [24] M. Bojowald, H. H. Hernandez, M. Kagan, P. Singh and A. Skirzewski, *Phys. Rev. D* **74** (2006) 123512 [arXiv:gr-qc/0609057].
- [25] M. Bojowald, *Gen. Rel. Grav.* **38** (2006) 1771 [arXiv:gr-qc/0609034].
- [26] A. Ashtekar and J. Lewandowski, *Class. Quant. Grav.* **14** (1997) A55 [arXiv:gr-qc/9602046].